Green Chemistry

PAPER

View Article Online
View Journal



Cite this: DOI: 10.1039/d5gc06663h

# Solvent-free synthesis of renewable FDCA-based bis-cyclic carbonate using a metal-free heterogeneous catalyst

Giovanni Berluti,[a] Angelo Scopano,[a] Gabriele Galletti,[a] Edwin Otten,[b] Coralie Jehanno[c] and Paolo P. Pescarmona *[a]

Received 9th December 2025,
Accepted 17th February 2026

DOI: 10.1039/d5gc06663h

rsc.li/greenchem

In this work, we developed a new catalytic strategy to synthesise an industrially relevant, fully renewable cyclic carbonate: 2,5-bis-dicarboxyl furan cyclic carbonate (BDFCC). This compound contains two terminal cyclic carbonate groups, which makes it attractive for application as a building block for green polymers. BDFCC was prepared from two renewable compounds: the methyl ester of 2,5-furandicarboxylic acid and glycerol carbonate, *via* a transesterification reaction at mild temperature (80 °C) using a novel, metal-free dual catalytic system consisting of commercially available ion-exchange resin beads (Amberlite IRA-900-Cl) and glycidol. Under conditions previously reported for homogeneous catalysis, involving *n*-hexane as solvent, only a moderate yield of BDFCC was achieved (42%). An improvement in both performance and sustainability of the process was achieved by implementing an equilibrium-shifting solvent-free strategy, which overcomes the thermodynamic limit of the reaction ($\Delta_r G°$ = +25 kJ mol$^{-1}$ based on DFT calculations). This approach, combined with an optimisation of the reaction conditions, allowed increasing the BDFCC yield to 86%. Furthermore, the heterogeneous resin bead catalyst was recyclable over multiple runs without experiencing loss of activity. Control experiments allowed to gain insight in the reaction mechanism and revealed the crucial role played by glycidol in promoting the catalytic activity of the Amberlite resin beads.



### Green foundation

1. Our work provides an innovative catalytic strategy to improve the synthesis of a renewable building block for green polymers by using a single-step, solvent-free route involving only renewable reactants and a reusable catalyst.
2. Our method allows preparing a useful product (2,5-bis-dicarboxyl furan cyclic carbonate, BDFCC) with 100% renewable carbon content, through a route with high atom efficiency (85%) and without requiring hazardous reactants used in previously reported work (such as thionyl chloride or *meta*-chloroperbenzoic acid). The sustainability of the process was further enhanced by understanding that the use of a fossil-derived solvent was not needed and by developing an equilibrium-shifting strategy based on using a $N_2$ flow to remove methanol.
3. Future research should aim at larger-scale synthesis with tailored reactor configurations for enabling the effective by-product removal that is necessary to circumvent the thermodynamic limit of this reaction.

## Introduction

Cyclic carbonates (CCs) are a class of green chemicals receiving increasing industrial interest for their low toxicity and broad range of applications. They can be used as monomers to produce polycarbonates, polyurethanes, polyesters or polyamines, or as solvents in Li-ion batteries, paints and coatings, dyes and personal care products.[1] As an additional attractive feature in the context of sustainability, they can be synthesised from $CO_2$, which is a low-cost, highly available industrial waste product, through a reaction with theoretical 100% atom efficiency. However, the remaining atoms constituting the cyclic carbonate molecule are generally still derived from fossil sources.[2] For this reason, growing interest has been directed to produce cyclic carbonates from bio-derived feedstock.[3,4] Among these bio-based cyclic carbonates, 2,5-bis-dicarboxyl furan cyclic carbonate (BDFCC) is particularly interesting because it contains two terminal cyclic carbonate groups

[a]*Chemical Engineering Group, Engineering and Technology Institute Groningen (ENTEG), University of Groningen, Nijenborgh 3, 9747 AG Groningen, The Netherlands. E-mail: p.p.pescarmona@rug.nl*
[b]*Stratingh Institute for Chemistry, University of Groningen, Nijenborgh 3, 9747 AG Groningen, The Netherlands*
[c]*POLYKEY POLYMERS, Gipuzkoa Science and Technology Park, Miramon Pasealekua 170, 20014 Donostia-San Sebastian, Spain*

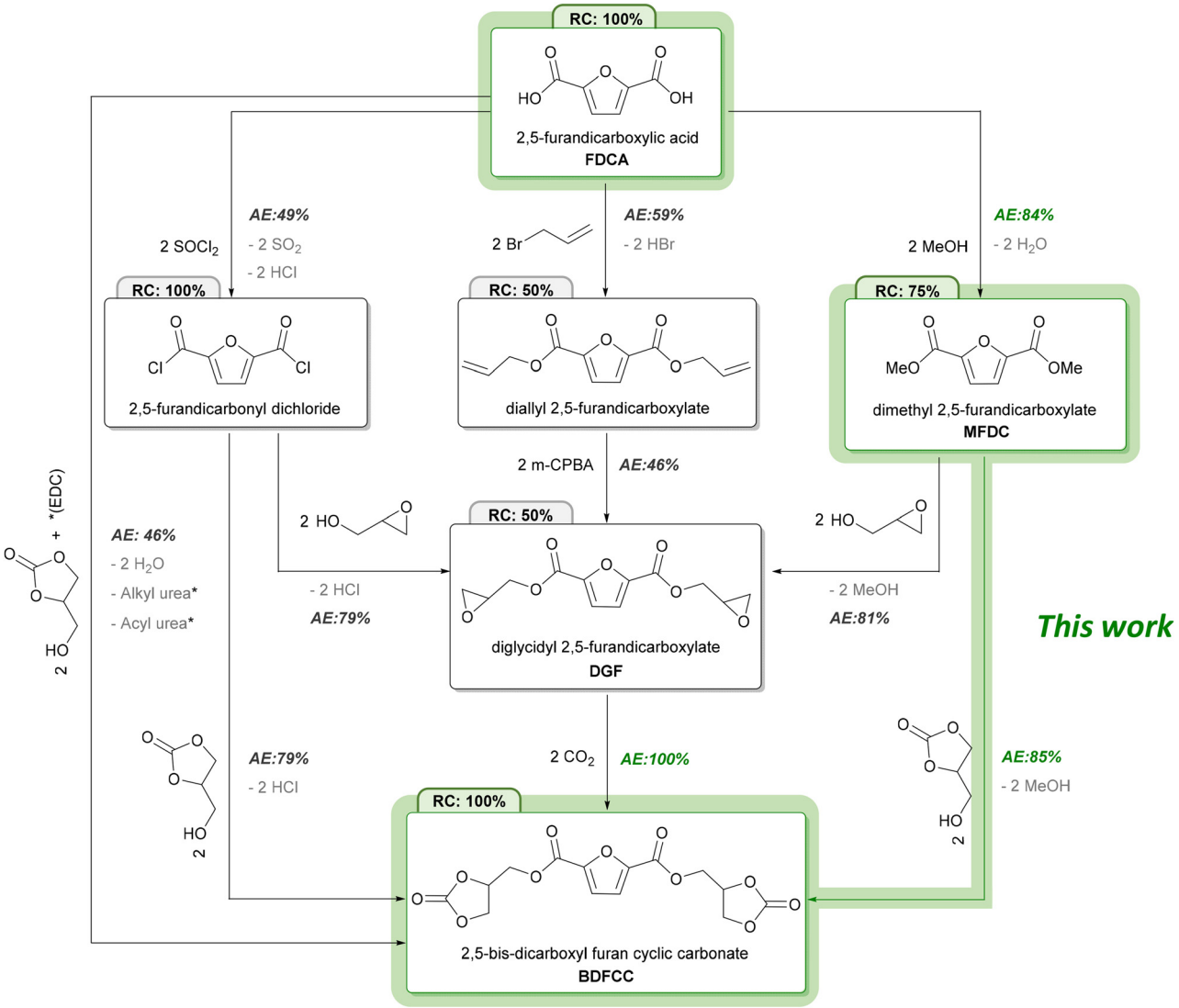


| | Allyl bromide | m-CPBA | EDC | MeOH | $SO_2$ | $SOCl_2$ | Glycidol | HCl | HBr |
|---|---|---|---|---|---|---|---|---|---|
| NFPA704 |  |  | NR |  |  |  |  |  |  |
| OEL | 0.1 ppm | NR | NR | 200 ppm | 0.25 ppm | 0.2 ppm | 2 ppm | 2 ppm | 2 ppm |



**Fig. 1** Reported synthetic pathways to produce BDFCC. *EDC: 1-ethyl-3-(3′-dimethylaminopropyl)carbodiimide hydrochloride, used in the catalytic mechanism (300 mol% relative to FDCA). *Alkyl and *acyl urea: side products deriving from EDC mechanism (see SI for the calculation of the renewable carbon content). AE: atom efficiency.

(Fig. 1). This feature is attractive for its application as a monomer for the production of non-isocyanate polyhydroxy urethanes (NIPHUs) and bisphenol A- or phosgene-free polycarbonates.[5–7] Therefore, BDFCC is considered promising to substitute substances that are currently used in the chemical industry but are classified as carcinogenic and mutagenic to reproduction (CMRs). BDFCC can be synthesised from 2,5-furandicarboxylic acid (FDCA) or its derivatives (Fig. 1). These compounds are characterised by a low tendency to undergo undesired side reactions leading to humins formation, which

instead plague other bio-based compounds such as 5-hydroxymethylfurfural.[7,8] Due to the recent realisation of up-scaled industrial production,[6] the use of FDCA as feedstock has increased its potential for applications.[9] These features are promising to enable the synthesis of BDFCC. However, there are only few studies in the literature reporting the synthesis of these bis-cyclic carbonates.[5,10–12] So far, four synthetic routes have been explored to prepare BDFCC (Fig. 1). In the work performed by L. Zhang *et al.*,[5] BDFCC was achieved from FDCA by a three-step synthesis. This route consisted in the formation of an allylic carbonyl intermediate using allyl bromide, followed by an epoxidation step using *meta*-chloroperbenzoic acid (*m*-CPBA) and the final carbonation using $CO_2$ and tetraethyl ammonium bromide (TEAB) as a catalyst. The same product was achieved in a different study using the acyl chloride derivative of FDCA, which was obtained by converting FDCA using $SOCl_2$.[10] Then, the esterification of this intermediate using glycerol carbonate (GlyC) and triethylamine as a catalyst yielded the target product. Similarly to this reaction route, in the studies performed by G. Shen *et al.*, the final cyclic carbonate was achieved starting from dimethyl 2,5-furandicarboxylate (*i.e.* the dimethyl ester of FDCA) by transesterification with glycerol carbonate catalysed by 4-dimethylaminopyridine (DMAP) in toluene.[11] The remaining synthetic route, developed by M. Eltayeb *et al*. focused on the direct conversion of FDCA and glycerol carbonate by Steglich esterification.[12] Due to its catalytic mechanism consisting in the cooperation between DMAP and 1-ethyl-3-(3′-dimethylaminopropyl)carbodiimide hydrochloride (EDC), this esterification allows using FDCA as a starting material without requiring a multi-step synthesis. All the routes described above rely on the use of homogeneous basic catalysts, and most of them require a multi-step synthesis and in some cases hazardous reagents (*e.g.* $SOCl_2$, *m*-CPBA). Such conditions inevitably generate waste, require extensive purification, and limit scalability, making them incompatible with the principles of green chemistry. To unlock the potential of BDFCC as a bio-based platform molecule, it is essential to develop simpler, safer, and more sustainable catalytic strategies to produce this compound. In particular, a single-step, solvent-free process using a recyclable heterogeneous catalyst would dramatically improve process intensification, reduce downstream separation, and offer a realistic path towards industrial-scale implementation. In this work we developed a novel dual catalytic system to enable the straightforward transesterification of the dimethyl ester of FDCA (dimethyl 2,5-furandicarboxylate, MFDC) and glycerol carbonate under mild conditions (80 °C, atmospheric pressure). Compared to the other routes in Fig. 1, our approach has the potential to be more sustainable, because: (i) it utilises two renewable starting materials as MFDC (a product of the sugar bio-refinery[6]) and glycerol carbonate (achievable from glycerol, a highly available and cheap by-product of the bio-diesel production,[13] and from $CO_2$ [14]); (ii) it does not require hazardous reagents as $SOCl_2$ or *m*-CPBA; (iii) it is carried out using an affordable, metal-free heterogeneous catalyst, (iv) in a solvent-free process. Furthermore, glycerol can also be used as feedstock in the production of glycidol,[15,16] making the chosen synthetic route fully renewable. In terms of green metrics,[17] the chosen synthetic pathway showcases high atom efficiency and renewable carbon content in comparison to the other routes reported in Fig. 1, while maximising the use of safe reactants.

# Experimental section

### Materials

Dimethyl 2,5-furandicarboxylate (MFDC, >98%), glycerol carbonate (GlyC, >90%), tris(2,4-pentanedionato)chromium(III) (>98%) and (±)-limonene (>95%) were purchased from Tokyo chemical industry (TCI). Amberlite IRA-900-Cl ion-exchange resin beads, glycidol (Gly, 96%), epichlorohydrin (>99%), 1,2-epoxy butane (99%), methanol (>99%), *n*-hexane (>99%), cyclohexane (>99%), isopropyl ether (99%), pentadecane (>99%), heptadecane (99%), dimethyl furan (99%), 2-methyl tetrahydrofuran (>99.5%), dimethyl sulphoxide (DMSO, >99%), *p*-cymene (99%), 1,3,5-trimethoxybenzene (>99%), and deuterated dimethyl sulphoxide ($d_6$-DMSO, >99%) were purchased from Sigma Aldrich.

### Catalytic tests

**Synthesis of BDFCC.** The catalytic tests were performed in 20 mL glass test tubes equipped with a magnetic stirrer and heated in an oil bath (see SI, Fig. S1).

In a typical catalytic test, MFDC (1.0 mmol), Amberlite IRA-900-Cl (30 mg), glycerol carbonate (2.2 mmol) and glycidol (0.4 mmol) were added in this order. Lastly, and if applicable, 0.5 mL of solvent was added to the previous mixture.

In a standard test carried out using a solvent under reflux, the test tube was connected to a 2 × 14/23 160 mm nozzle condenser cooled by water. Most tests were performed at 80 °C and stirred at 450 rpm for the selected reaction time, though also a lower reaction temperature (60 °C) was explored (see SI, Fig. S2). When solvent-free conditions were adopted, no solvent was added to the mixture and different set-up configurations were explored employing or not a gas carrier (see SI). At the end of each test, the supernatant solvent (when added) was separated from the crude mixture, followed by purification from solvent residues by vacuum-evaporation. Afterwards, trimethoxy benzene (1.8 mmol) was added to the reaction mixture as internal standard for NMR spectroscopy quantification, and approximately 2.5 mL of $d_6$-DMSO was added to solubilise the mixture. The test tube was kept under stirring at 450 rpm and 80 °C until complete dissolution (2 to 3 min). When the experiments led to high yields, highlighted by the presence of a large amount of a white solid, the solubilisation was achieved using the double of the amount of $d_6$-DMSO, using a heat gun to help dissolve the solid and, if necessary, by manual stirring. Once a homogeneous solution was achieved, 0.6–0.7 mL of diluted reaction mixture was collected for the $^1$H-NMR analysis. Quantitative $^{13}$C-NMR was conducted by collecting approximately 0.5–0.7 mL of the same solution and then adding 5–6 mg of chromium(III) acetyl acetonate

used as a relaxing agent for the $^{13}$C-NMR analysis. Quantitative $^{1}$H-NMR (600 MHz) and $^{13}$C-NMR (150 MHz) spectroscopy were used in combination to quantify the conversion, yield and selectivity (see section on NMR quantification in the SI for details about the calculation). The resulting files (FID format) were analysed and processed using the software "MestReNova" v15.0.0–34764.

**Reproducibility tests.** Each of the tests of the target reaction at 2, 7, and 24 h, either with *n*-hexane or in a solvent-free system, was carried out at least in triplicate, to evaluate the reproducibility of the results. The average and standard deviation calculated from the results of these tests are shown in Fig. 2a and b. These tests demonstrated a good degree of reproducibility, particularly when taking into account the complexity of the quantification of the reaction products, which give overlapping $^{1}$H-NMR signals (see section on NMR quantification, SI).

**DFT calculations.** The standard Gibbs free energy of MFDC, glycerol carbonate, BDFCC and methanol (see SI, Fig. S3–S5, Tables S1–S4) were calculated using the Gaussian 16, Revision B.01 program. The following parameters were adopted for the calculation: method: B3LYP; basis set: def2TZVP; empirical dispersion: GD3. Geometry optimisations were performed in the gas phase. The optimised structures correspond to a true minimum on the potential energy surface based on a frequency analysis (no imaginary frequencies). Solvation energies were obtained from a single-point energy calculation on the gas phase geometries using an SMD continuum model (solvent: DMSO).

**Catalyst recyclability test.** The recyclability test of the catalyst was performed in the $N_2$-flow configuration under specific solvent-free reaction conditions (see SI). This allowed preventing the embrittlement of the Amberlite beads that was observed after multiple runs if a 10 × 6 mm magnetic rod was used as stirring element and the beads were washed in acetone and dried at 80 °C. At the end of the first catalytic run the reaction mixture was collected to perform further NMR spectroscopy analysis using a 120 × 0.8 mm syringe, while avoiding the removal of the catalyst beads. Then, 2 mL of MeTHF was added into the vial to wash away residual reactants adsorbed on the beads. The solvent was then removed with a syringe, and the solid catalyst was dried by purging the vial with an air flow through a needle. After this step, the starting reagents besides the Amberlite IRA-900-Cl beads were loaded into the vial. This procedure was repeated over five consecutive runs (see SI, Table S5). A recyclability test without the reintroduction of glycidol was performed following the same procedure described above (see SI, Fig. S6).

**Upscaled synthesis of BDFCC.** For a 3.0 g production of BDFCC, a 50 mL glass vial was loaded with MFDC (0.02 mol), glycerol carbonate (0.2 mol), Amberlite IRA-900-Cl (16 wt% relative to MFDC) and glycidol (40 mol% relative to MFDC), respectively (see SI, Fig. S7). The reaction was performed at 80 °C under a constant $N_2$ flow of 55 mL min$^{-1}$ and stirred at 450 rpm, until complete conversion of MFDC to BDFCC, as determined based on the depletion of the ester peak (–OMe) at 3.9 ppm in the $^{1}$H-NMR spectrum (>95% after 66 h). To isolate BDFCC, which is a solid at the end of the reaction, the sample was dissolved in acetone. The catalyst beads were easily removed by filtration through a plastic sieve (mesh size: 0.5 mm). The filtered solution was then concentrated by vacuum evaporation, after which the precipitation of the solid BDFCC was achieved by rapidly adding cold water (40 mL). After this, the solid was separated from the liquid mixture by vacuum filtration on a Buchner filter. The recovered liquid fraction was cooled down to approximately 0 °C, allowing precipitation of an additional amount of BDFCC, which was then recovered by vacuum filtration. This treatment at 0 °C was repeated a second time. After this, the solid fractions were merged, washed with cold water (20 mL) to remove possible traces of glycerol carbonate and separated from the liquid by vacuum filtration (this washing procedure was repeated 4 times). The same procedure was repeated in a different test using Ar as a gas carrier, yielding the same results and proving Ar to be interchangeable with $N_2$. For a 7.0 g production of BDFCC, a 100 mL round bottom flask was loaded with

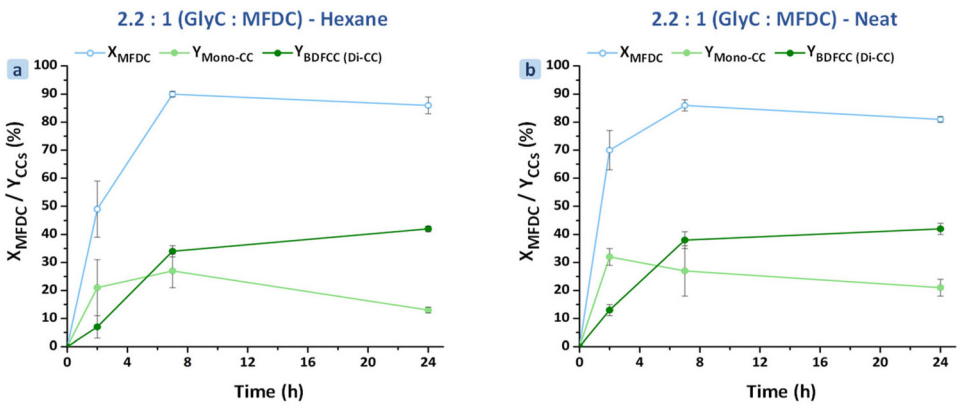


**Fig. 2** Synthesis of BDFCC as a function of reaction time, with *n*-hexane or in a solvent-free system. Conditions: (a) MFDC (1.0 mmol), GlyC (2.2 mmol), Amb IRA-900-Cl (30 mg), Gly (0.4 mmol), *n*-hexane (0.5 mL), reflux. (b) MFDC (1.0 mmol), GlyC (2.2 mmol), Amb IRA-900-Cl (30 mg), Gly (0.4 mmol), no solvent, 80 °C, $N_2$ flow (10 mL min$^{-1}$). Each experiment was performed at least in triplicate.

0.04 mol of MFDC and the other reagents respecting the same ratios as in the 3.0 g production of BDFCC. The reaction was performed at 80 °C, under a constant moderate Ar flow and left stirring for 24 h while monitoring the conversion of MFDC to BDFCC by $^1$H-NMR spectroscopy (>90% after 24 h). At the end of the reaction, the same purification process previously described was performed yielding BDFCC with a purity of >90%.

**Products identification.** The separation and identification of the main transesterification products was performed by column chromatography followed by analysis by NMR spectroscopy (Fig. S9–S19). The main products of the reaction *i.e.* Mono-CC and BDFCC (Di-CC) were then characterised by Fourier Transform infrared (FT-IR) spectroscopy (Fig. S20). The spectra were recorded between 4000 and 500 $cm^{-1}$ using the attenuated total reflectance technique (ATR) on a IRTracer-100 spectrometer by averaging 64 scans with a spatial resolution of 4 $cm^{-1}$ using the Happ-Genzel apodisation method.

**Amberlite resin beads characterisation.** The fresh Amberlite IRA-900-Cl resin beads were characterised by FT-IR spectroscopy (Fig. S21) using the method described above. The surface morphology of the resin beads (previously coated with gold to increase the conductivity) was investigated by scanning electron microscopy (SEM) using a Nova NanoSEM 650 microscope (Fig. S22a–c). The thermal stability of the resin beads was investigated by thermogravimetric analysis (TGA) under air from 35 to 750 °C with a ramp of 10 °C $min^{-1}$ using a thermogravimetric analyser TGA-550 (Fig. S23).

## Results and discussion

### Synthesis of BDFCC

In the first step of this work, the transesterification of MFDC with glycerol carbonate to synthesise BDFCC was explored using commercial Amberlite IRA-900-Cl resin beads as a heterogeneous catalyst. These resin beads consist of a porous cross-linked network of polydivinyl benzene and polystyrene with tetrasubstituted ammonium groups with chloride ions as the counter anions (see SI, Fig. S21 and S22 for characterisation by FT-IR and SEM). The $Cl^-$ content of these beads was previously determined to be 3.83 $mmol_{Cl}$ $g^{-1}$.[18] TGA indicated that the resin beads start to undergo thermal degradation well above 200 °C (see SI, Fig. S23). This means that they are expected to be stable in the temperature range in which they are generally employed (<100 °C), and in which our study was also performed. The initial catalytic tests were carried out at 80 °C, based on the conditions used in previous studies for transesterification reactions employing *n*-hexane as solvent.[19] Under these conditions, the Amberlite IRA-900-Cl showed negligible activity for the target transesterification, resulting in no cyclic carbonate-functionalised furanic products (Table 1, entry 1). We attributed the inactivity of the Amberlite to the weak Brønsted basicity of the chloride moieties, making them unsuitable for deprotonating glycerol carbonate and thus initiate the transesterification. To tackle this issue, we introduced glycidol as a second component of the catalytic system. Glycidol can form an anionic chlorohydrin intermediate upon nucleophilic attack by halides (and indeed chlorohydrin was identified by $^1$H-NMR analysis of a fraction separated by column chromatography from the crude of reaction, see SI Fig. S15),[20] which has been shown to possess sufficient basicity to enable deprotonation and activate transesterification reactions.[21] Our strategy proved effective, and the enhanced dual catalytic system consisting of Amberlite IRA-900-Cl (30 mg) in combination with glycidol (40 mol% relative to MFDC) yielded a mixture of the mono-substituted cyclic carbonate (Mono-CC) and the di-substituted cyclic carbonate (BDFCC), which precipitated from the reaction mixture as a white crystalline solid ($X_{MFDC}$ = 90%, $Y_{BDFCC}$ = 34% and $Y_{Mono\text{-}CC}$ = 27% after 7 h at 80 °C, see Fig. 2a). Side-products were also obtained, *i.e.* the mono-substituted epoxy product (Mono-Ep), generated through the nucleophilic attack of glycidol on one side of MFDC, and the epoxy-carbonate-substituted product (Ep-CC) (see SI, Table S6, entry 1, 7 h). The latter is a potentially relevant product too, as its two different functional groups can be attractive for application as a monomer for polymer synthesis. The results of this catalytic test suggest a mechanism in which the chlorides contained in the Amberlite IRA-900-Cl activate glycidol *via* formation of an anionic chloro-

**Table 1** Contribution of the components of the catalytic system to the activity. Conditions: MFDC (1.0 mmol), GlyC (2.2 mmol), Amb IRA-900-Cl (30 mg, when employed), epoxide (0.4 mmol, when employed), no solvent, 2 h, 80 °C, 10 ml $min^{-1}$ of $N_2$ (when used); n.a. = not applicable. The test in a closed system (entry 5) was performed in duplicate (the average values are reported). The test under $N_2$ flow (entry 8) was performed in quadruplicate (the average values are reported). See SI for details on the epoxide mole balance calculation

| Entry | Catalytic component | Set-up | $X_{MFDC}$ | $Y_{Mono\text{-}CC}$ | $Y_{BDFCC}$ | $Y_{Mono\text{-}Ep}$ | $Y_{Ep\text{-}CC}$ | Epoxide mole balance |
|---|---|---|---|---|---|---|---|---|
| 1 | Amb IRA-900-Cl | Closed | 3 | 0 | 0 | 0 | 0 | n.a. |
| 2 | Glycidol (Gly) | Closed | 11 | 5 | 0 | 5 | 0 | 91% |
| 3 | Epichlorohydrin (ECH) | Closed | 3 | 0 | 0 | 0 | 0 | 55% |
| 4 | Butylene oxide (BO) | Closed | 3 | 0 | 0 | 0 | 0 | 28% |
| 5 | Gly + Amb IRA-900-Cl | Closed | 23 | 9 | 2 | 6 | 0 | 65% |
| 6 | ECH + Amb IRA-900-Cl | Closed | 14 | 10 | 1 | 0 | 0 | 60% |
| 7 | BO + Amb IRA-900-Cl | Closed | 9 | 5 | 0 | 0 | 0 | 25% |
| 8 | Gly + Amb IRA-900-Cl | $N_2$ flow | 70 | 32 | 13 | 9 | 6 | 71% |
| 9 | ECH + Amb IRA-900-Cl | $N_2$ flow | 14 | 10 | 0 | 0 | 0 | 35% |
| 10 | BO + Amb IRA-900-Cl | $N_2$ flow | 6 | 0 | 0 | 0 | 0 | 0% |

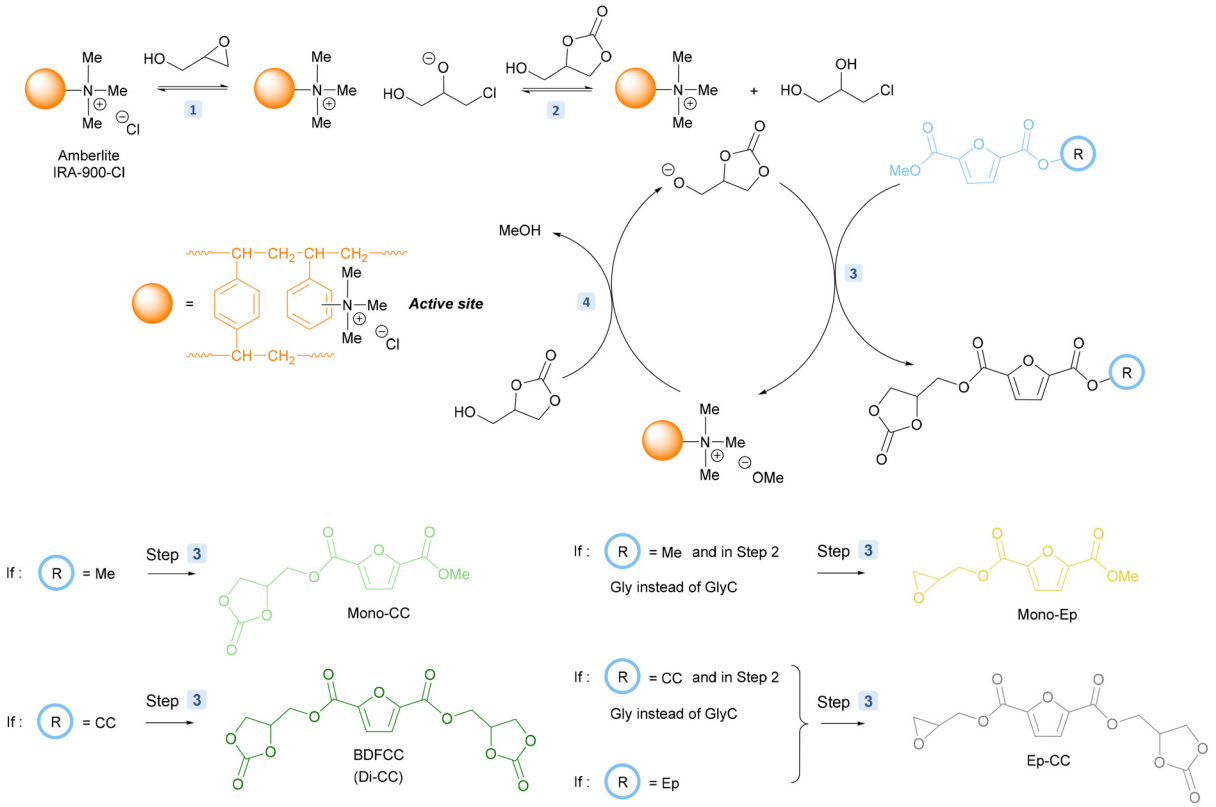


**Scheme 1** Proposed mechanism for the transesterification of MFDC and GlyC catalysed by Amberlite IRA-900-Cl in cooperation with glycidol. Functional groups: Me: methyl, CC: cyclic carbonate and Ep: epoxy.

hydrin intermediate (Scheme 1, Step 1). This step is followed by deprotonation of glycerol carbonate (Step 2), which enables its reaction with the starting MFDC (Step 3). The methoxide leaving groups, being strong Brønsted bases, are also expected to take part in the deprotonation of glycerol carbonate (Step 4), sustaining the transesterification process and yielding methanol as a by-product, as observed by $^{1}$H-NMR spectroscopy (Fig. S18). The formation of the epoxy-substituted side-products indicates that the deprotonation of glycidol competes with that of glycerol carbonate (Scheme 1, Step 2). Indeed, glycidol has been already used for the direct transesterification and esterification of FDCA-derivatives to produce DGF *via* homogeneous basic catalysis (Fig. 1).[19,22,23] To further explore the products distribution of this reaction, other tests with a duration of 2 and 24 h were performed (Fig. 2a). These tests highlighted that Mono-CC acts as an intermediate that reaches a maximum yield after 2 h, after which its concentration declines due to its conversion into BDFCC. The yield of BDFCC reached 42% after 24 h. The summed yield of the Mono-Ep and Ep-CC species after 24 h (Table S6, entry 1, 24 h) did not change significantly compared to the values observed after 7 h.

### Solvent effect and equilibrium-shifting strategy

While the results reported so far demonstrate that Amberlite IRA-900-Cl in combination with glycidol is an effective catalytic system for the synthesis of BDFCC, it only reaches moderate yield of the desired bis-carbonated product, and it relies on the use of *n*-hexane as solvent. Due to its fossil origin, high volatility, flammability, environmental impact and risk for health, a greener alternative to *n*-hexane is desirable.[24–26] For this purpose, an initial screening of different solvents to replace *n*-hexane was performed. Two main criteria were considered in the selection: (i) protic solvents were discarded due to their possible reactivity under the alkaline reaction conditions, which would be detrimental for the reaction selectivity; (ii) potentially renewable, bio-based alternatives were chosen, *i.e.* heptadecane, pentadecane, limonene, *p*-cymene, 2-methyl tetrahydrofuran and 2,5-dimethyl furan. However, fossil-derived solvents such as cyclohexane, diisopropyl ether and dimethyl sulphoxide were also used in these studies as a comparison to *n*-hexane. A low level of toxicity was also targeted, with 2-methyl tetrahydrofuran and 2,5-dimethyl furan being preferable in this sense. Notably, this screening proved that the nature of the solvent has a major role on the MFDC conversion and products yields (Fig. 3). *N*-hexane gave the best results, whereas polar compounds such as 2,5-dimethylfuran, 2-methyl tetrahydrofuran, and dimethyl sulphoxide were detrimental for the formation of the Mono-CC and BDFCC products. We observed that the initial reaction mixture was monophasic when the more polar solvents were employed, whereas it was biphasic with the less polar solvents that are not misci-

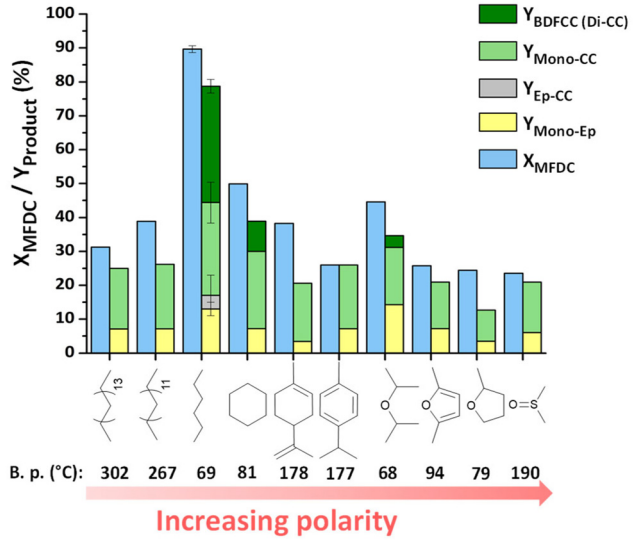


**Fig. 3** Effect of the type of solvent on the transesterification of MFDC with GlyC. Conditions: MFDC (1.0 mmol), GlyC (2.2 mmol), Amb IRA-900-Cl (30 mg), Gly (0.4 mmol), solvent (0.5 mL), 7 h, 80 °C (under reflux for *n*-hexane, cyclohexane, isopropyl alcohol and 2-methyl tetrahydrofuran). The polarity order was defined based on the dielectric constant values of the solvents.

ble with the solution of MFDC (a solid at room temperature) in GlyC. This suggests that the role of the compound used as a solvent is actually not to help form a homogeneous mixture with the reactants. We reasoned that the role of the apolar solvent is rather that of helping the removal of methanol formed during the reaction (Scheme 1) from the phase containing the reactants and products. Transesterification, similarly to esterification, is a class of reactions generally characterised by close to neutral enthalpy and entropy differences.[27] This implies that equilibrium-shifting strategies are required to reach a high yield of the product. In this context, an apolar compound that does not mix with the reactants but forms a low boiling mixture with methanol would tend to vaporise and recondense in the reflux setup used in these tests, whereas the methanol that is vaporised together with it would be largely removed being more volatile. In turn, this would shift the equilibrium concentrations towards the products. This hypothesis explains well our results (Fig. 3), which showed that the highest conversion and product yields were obtained with the lowest-boiling among the apolar solvents (*n*-hexane), followed by the second lowest-boiling apolar solvent (cyclohexane). Polar solvents form a single phase with the reactants, and the obtained mixture is expected to have a higher boiling point than the solvent alone since GlyC and MFDC have very high boiling points. This limits the reflux and thus the removal of the formed methanol from the reaction mixture. Combining these considerations, it can be concluded that both low boiling point and apolarity promote the conversion and products yields. Taking these two parameters into account, the trends observed in Fig. 3 can be understood. With the purpose of removing methanol in a more effective way and at the same time to increase the sustainability of the process, we omitted *n*-hexane from the reaction and instead we explored different solvent-free strategies (neat reactions). Three different set-up configurations were explored: a solvent-free reaction in (i) a closed vessel, (ii) an open vessel and (iii) in an open vessel under $N_2$ flow (Fig. S1). The extent of methanol removal was calculated by $^1$H-NMR spectroscopy (see section on NMR quantification in the SI for details on the calculation). In line with logical expectations, most of the methanol remained in the system when the closed-vessel configuration was used (16% loss, see Fig. 4), whereas a large fraction of the methanol was removed in the open-vessel configuration (93% removal) and virtually complete removal was achieved in the gas-flow configuration (>99% removal). The yield and selectivity towards the target BDFCC improved significantly with increasing degree of methanol removal (Fig. 4), reaching 86% conversion of MFDC with 27% yield of Mono-CC and 38% yield of BDFCC in 7 h of reaction at 80 °C under $N_2$ flow (Fig. 4). When carrying out the catalytic test under $N_2$ flow at different reaction times (Fig. 2b), the performance was similar yet slightly better compared to that in the presence of *n*-hexane, both in terms of summed yield and selectivity towards the carbonated furanic products (compare $Y_{Mono\text{-}CC}$ and $Y_{BDFCC}$ values at the different reaction times in Fig. 2a and b). Besides the target carbonated furanic products, we also observed the formation of a small amount of the Mono-Ep and Ep-CC side products (see SI, Table S6, entry 2).

Furthermore, a test was performed at 60 °C using the open vessel configuration under $N_2$ flow, leading to markedly lower conversion and a very low yield of BDFCC (6% after 7 h of reaction) despite a similar degree of methanol removal (see SI, Fig. S2). Therefore, 80 °C was selected as temperature for further investigation of the transesterification of MFDC with GlyC.

## DFT calculations

To corroborate that the transesterification of MFDC with GlyC is a thermodynamically-limited reaction as postulated, density functional theory (DFT) calculations using the Gaussian soft-

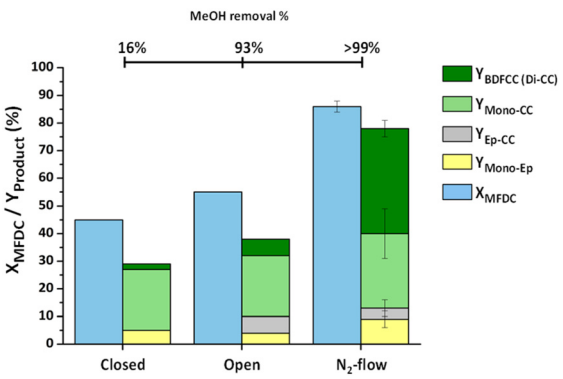


**Fig. 4** Studies on methanol removal using different set-up configurations. Conditions: MFDC (1.0 mmol), GlyC (2.2 mmol), Amb IRA-900-Cl (30 mg), Gly (0.4 mmol), 7 h, no solvent, 80 °C, 10 ml min$^{-1}$ of $N_2$ ($N_2$-flow system). The test under $N_2$ flow was performed in triplicate.

ware were performed to determine the thermodynamic parameters for MFDC, GlyC, methanol and BDFCC (see SI, Fig. S3 and S4, Tables S1–S4). In this calculation, the molecular geometry of each compound in the gas-phase was optimised at the B3LYP/def2TZVP level of theory including the Grimme's D3 empirical dispersion method to improve the description of the van der Waals and London dispersion forces (see SI for further details).[28] A frequency analysis confirmed the structures to be minima on the potential energy surface, and provided thermochemical data. This calculation surprisingly led to a large positive Gibbs free energy of +27 kJ $mol^{-1}$ for our reaction (Fig. S3, Table S2), which is significantly larger than what is commonly expected for transesterifications,[29] and which indicates that the reaction is thermodynamically unfavourable. This Gibbs free energy value stems from a very low total difference in entropy of −0.001389 kJ $mol^{-1}$ and to a more significant difference in enthalpy of +23 kJ $mol^{-1}$. This indicates that the unfavourable thermodynamics of the transesterification of MFDC to BDFCC originates from the relatively high enthalpy of the products. We subsequently took the gas phase geometries and performed a single-point energy calculation using the SMD continuum model to obtain the solvation energies of all species, utilising DMSO as a model solvent.[30] Under these conditions, a change in Gibbs free energy of +25 kJ $mol^{-1}$ was calculated for the transesterification of MFDC and GlyC in liquid phase (Table S3), indicating a small stabilisation of the products due to solvation. Using the $\Delta_r H°$ and $\Delta_r S°$ calculated by DFT at 298 K in DMSO, and assuming them to be independent of temperature, we calculated a $\Delta_r G_{353.15K}$ = +26 kJ $mol^{-1}$ (*i.e.* at the reaction temperature of 80 °C), and from this we calculated an equilibrium constant of $K_{eq}$ = 0.0001 (Table S4). Using this $K_{eq}$ value with the employed reactant ratio GlyC/MFDC = 2.2, a conversion at equilibrium of $X_{MFDC,\ eq,\ 353K}$ = 5% is obtained. This value is significantly lower than the conversion of MFDC that we observed experimentally in the test in DMSO at 80 °C for 7 h (24%, see Fig. 3), which would correspond to a $\Delta_r G_{353.15K}$ = +11 kJ $mol^{-1}$ assuming that equilibrium was reached within the 7 h of reaction. However, at the temperature of reaction (80 °C), methanol evaporation cannot be avoided due to its low boiling point ($T_b$ = 65 °C), and thus a higher degree of conversion than the one predicted by DFT can be expected. To circumvent this issue, we tested the reverse reaction, *i.e.* the methanolysis of BDFCC into MFDC and GlyC, performed using a ratio methanol/BDFCC = 2. This test led to 89% conversion of BDFCC after 24 h, which did not increase if the reaction was extended to 92 h (Fig. S5). This value is in satisfactory agreement with the theoretical conversion at equilibrium (95%) calculated considering a $\Delta_r G_{353.15K}$ = −26 kJ $mol^{-1}$. These results confirm that the transesterification of MFDC and GlyC is thermodynamically limited, underlining that methanol removal is crucial to obtain good yields of the desired BDFCC product.

### Solvent-free synthesis optimisation

After understanding the key role of methanol removal in shifting the chemical equilibrium and improving the sustainability of the reaction, the conditions for the systems under $N_2$ flow were optimised to achieve higher BDFCC yields. While the new $N_2$-flow system proved more effective than the system using *n*-hexane, with none of the two full conversion of MFDC into BDFCC was achieved after 24 h of reaction (Fig. 2a and b). Moreover, in both cases the selectivity of the reaction was affected by the formation of the Mono-Ep and Ep-CC side products. The combined yield of these species remained approximately steady throughout the experiment, with a gradual increase in the Ep-CC-to-Mono-Ep ratio as the reaction proceeded for 24 h (see SI, Table S6, entry 2). We reasoned that these limitations are probably caused by two main factors: (i) the only slight excess of GlyC (1.1 eq.) relative to MFDC; (ii) the partial solidification of the reaction mixture observed after 7 h under these conditions. The former can limit the reactivity due to a lack of reactants, according to Le Chatelier's principle. The latter can physically limit the mobility of GlyC and MFDC in the reaction mixture. Specifically, the solidification of the reaction mixture was always observed when high yields of Mono-CC and BDFCC were achieved (after 4 h using a 2.2 : 1 ratio of GlyC : MFDC), due to the low remaining amount of glycerol carbonate able to dissolve them (and MFDC). Therefore, aiming at higher yield of BDFCC, different ratios of GlyC : MFDC were explored using the novel solvent-free conditions (Fig. 5a and b). The use of a larger excess of GlyC provided a monophasic solution in which the Mono-CC and BDFCC products dissolve even when obtained at higher yields.

This resulted in a system in which GlyC and MFDC reactivity is preserved. Additionally, the excess of GlyC is anticipated to increase products yields based on Le Chatelier's principle. The results achieved using the GlyC : MFDC ratios of respectively 4.4 : 1 and 10 : 1 showed the expected increase in the yields of cyclic carbonates over time, as well as of the selectivity towards BDFCC (compare Fig. 2b, 5a and b). Employing GlyC : MFDC = 10 : 1, nearly full conversion (95%) of MFDC with a very high yield (86%) and selectivity (90%) of BDFCC were reached after 24 h (Fig. 5b). As an additional benefit, using a 10 : 1 ratio of GlyC significantly limited the formation of the side products originating from the reaction of MFDC with glycidol. After 24 h of reaction, the yields of Mono-Ep and Ep-CC were negligible (<1%) while a 15% yield of Mono-Ep was observed in the initial phase of the test (Table S6, entry 4). These results can be understood considering the competition between GlyC and glycidol in Step 2 in Scheme 1 (*vide supra*). The higher relative amount of GlyC limits the deprotonation of glycidol, decreasing the formation of Mono-Ep and Ep-CC, and favours their conversion into Mono-CC and BDFCC, with glycidol as a leaving group.

In an attempt to further improve the process, different types of carrier gases and flows rates were studied and the methanol removal extent was compared (Fig. 6a and b). Among the gas flows tested to promote the reaction, nitrogen and air showed the best performance as almost complete stripping of the reaction by-product was achieved, (Fig. 6a, >95% methanol removal). On the contrary, using $CO_2$ resulted in lower yield of Mono-CC and BDFCC despite the similarly high

 

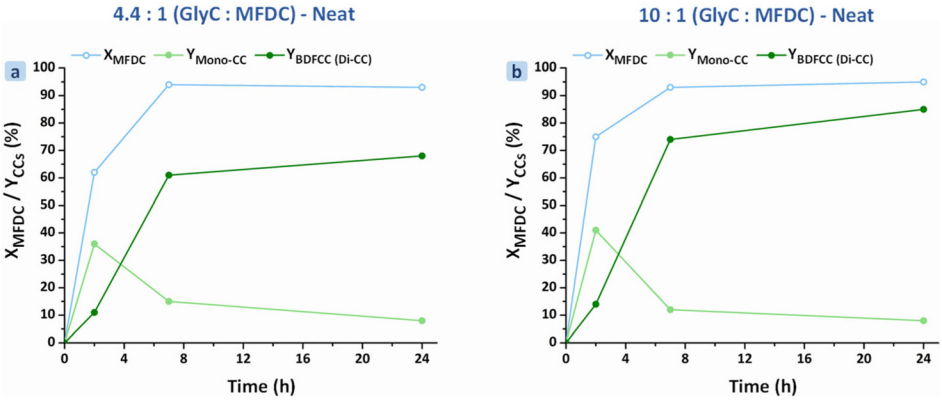


**Fig. 5** Synthesis of BDFCC as a function of reaction time, in a solvent-free system with different GlyC : MFDC ratios. Conditions: (a) MFDC (1.0 mmol), GlyC (4.4 mmol), Amb IRA-900-Cl (30 mg), Gly (0.4 mmol), no solvent, 80 °C, $N_2$ flow (10 mL $min^{-1}$). (b) MFDC (1.0 mmol), GlyC (10 mmol), Amb IRA-900-Cl (30mg), Gly (0.4 mmol), no solvent, 80 °C, $N_2$ flow (10 mL $min^{-1}$).

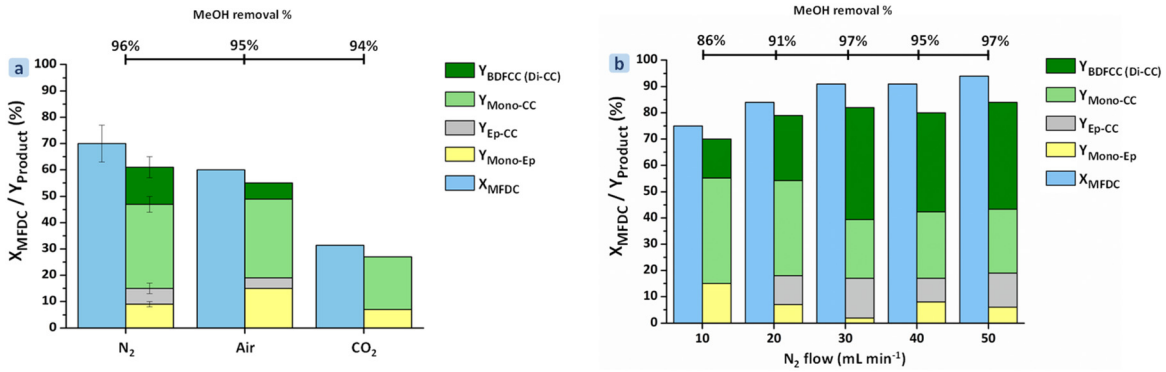


**Fig. 6** Studies on methanol removal using: (a) different type of gas carrier and (b) different $N_2$ flows. Conditions: (a) MFDC (1.0 mmol), GlyC (2.2 mmol), Amb IRA-900-Cl (30 mg), Gly (0.4 mmol), no solvent, 2 h, 80 °C, 10 mL $min^{-1}$ of gas. The test under $N_2$ flow was performed in quadruplicate. (b) MFDC (1.0 mmol), GlyC (10 mmol), Amb IRA-900-Cl (30 mg), Gly (0.4 mmol), no solvent, 2 h, 80 °C.

degree of methanol removal (Fig. 6a). We hypothesise that this is due to glycidol consumption through its reaction with $CO_2$. Indeed, glycidol is known to react with $CO_2$ in the presence of halide-based catalysts to produce glycerol carbonate.[31,32] As a consequence, less glycidol would be available to act as initiator of the catalytic mechanism for the reaction of MFDC with GlyC (Step 1 in Scheme 1). After concluding that nitrogen and air flows are the most suitable options to promote the reaction, nitrogen was chosen for follow-up tests, as the presence of oxygen in the gas might result in oxidation side reactions at longer reaction times. Different nitrogen flows were then tested (after 2 h of reaction), showing an increasing selectivity towards the BDFCC product by increasing the gas flow from 10 to 50 mL $min^{-1}$ (Fig. 6b). This trend can be explained by the increased efficiency of methanol removal with increasing the gas flow. 30 mL $min^{-1}$ was selected as the optimal gas flow, as a trade-off between maximising the selectivity towards the carbonated furanic products and minimising gas consumption.

With the developed set-up configuration, recyclability tests were performed using the optimised GlyC : MFDC ratio and $N_2$ flow. The catalyst was recycled four times, demonstrating a constant conversion and selectivity over 5 consecutive runs (Fig. 7). Glycidol reintroduction with the starting materials was found to be critical to keep the activity of the system (see SI, Fig. S6).

## Understanding the contribution of the components of the catalytic system

To gain further insight into the contribution of each component of catalytic system to the observed overall activity, a series of systematic control experiments was performed. Each component was individually investigated at 80 °C for 2 h, using a ratio of GlyC : MFDC of 2.2 : 1 and using a closed-vessel or a $N_2$-flow configuration (Table 1). As previously discussed, Amberlite IRA-900-Cl alone in a closed-vessel showed negligible activity for the transesterification of MFDC (Table 1, entry 1). This can be explained considering that the chloride anions contained in the Amberlite beads are weak Brønsted bases and are thus not expected to be able to deprotonate the hydroxyl group of glycerol carbonate. On the other hand, testing glycidol alone resulted in a low but measurable MFDC conversion, with Mono-CC and Mono-Ep as the products, each

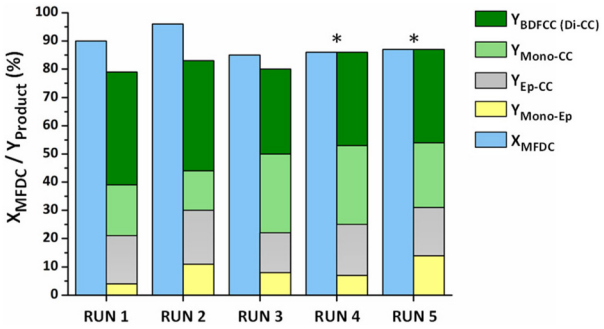


**Fig. 7** Recyclability test. Conditions: MFDC (1.0 mmol), GlyC (10 mmol), Amb IRA-900-Cl (30 mg), Gly (0.4 mmol), no solvent, 2 h, 80 °C, 30 ml $min^{-1}$ of $N_2$ flow. *The summed yield of the products in the last two runs was slightly higher than the conversion of MFDC. This suggests a positive error in $^{13}C$-NMR and $^{1}H$-NMR quantification at the reaction conditions used. Thus, for these tests the product yields were normalised so that their sum is 100% (see SI, Table S5).

in 5% yield (Table 1, entry 2). This result could be considered surprising, since no chlorohydrin anionic intermediate can be formed without a nucleophilic species as the chloride provided by the Amberlite IRA-900-Cl. This suggests that glycidol is able to act as a nucleophile in the transesterification of MFDC. This behaviour might be related to the proposed tendency of glycidol to form resonance structures in which the epoxide ring opens and then forms again using the O atom in the hydroxyl group, through a proton-transfer mechanism.[33] To test if this effect is specific to glycidol, epoxides without a hydroxyl group, such as epichlorohydrin (ECH) and butylene oxide (BO), were tested under the same conditions. These control experiments resulted in negligible yields of carbonated furanic products. On the other hand, when tested in cooperation with the Amberlite resin catalyst, all epoxides led to the formation of carbonated furanic products (Table 1, entries 5–7), supporting the proposed role of the formation of the anionic chlorohydrin intermediate in the transesterification mechanism (Scheme 1). It is worth noting that with ECH and BO, only carbonated products were observed (mainly Mono-CC, entries 6 and 7), whereas glycidol led to a significant amount of Mono-EP side product (entry 5), due to its self-deprotonation and to the deprotonation in Step 2 of Scheme 1. Although these results should be discussed only in a qualitative way as evaporation of ECH (b.p. 117 °C) and particularly of BO (b.p. 65 °C) were observed despite the use of a close-vessel configuration (see epoxide mole balance in Table 1), they clearly point to a different behaviour between glycidol and the other epoxides that do not contain the vicinal hydroxyl group.

To investigate the effect of a gas flow on the reaction system, the same studies were repeated under $N_2$ flow. In line with the trend observed in the closed-vessel configuration, the best catalytic performance was achieved when the Amberlite beads were used in combination with glycidol. Under these conditions, besides removing methanol, the gas flow led to a significant epoxide evaporation, particularly when ECH and BO were used (see epoxide mole balance in Table 1). On the other hand, the use of gas carrier proved crucial to boost the performance of the reaction by circumventing the thermodynamic limit (*vide supra*). Combining these observations, we conclude that the high boiling point (167 °C) and resonance structures of glycidol make this compound the most effective epoxide species for promoting the transesterification of MFDC with GlyC at the solvent-free conditions developed in this work.

Next, the most effective catalytic system consisting of Amberlite IRA-900-Cl and glycidol was tuned by screening different concentrations of the two components (Fig. 8). When keeping the amount of Amberlite IRA-900-Cl fixed and varying that of glycidol, the best performance was observed at intermediate amount of glycidol (20 mol% relative to MFDC, see Fig. 8a). This can be rationalised considering that glycidol plays a catalytic role in this system, but if its relative amount becomes too high it starts to compete with glycerol carbonate in the transesterification reaction, thus leading to an increased selectivity towards the epoxy-functionalised products (Mono-Ep and Ep-CC, see Fig. S8, SI). Also in the tests in which the amount of glycidol was kept constant and that of Amberlite IRA-900-Cl varied (Fig. 8b), the optimum catalytic performance was observed at intermediate values, *i.e.* with a glycidol-to-chloride ratio of 1.7 (see SI, Tables S7 and S8). A lower glycidol-to-

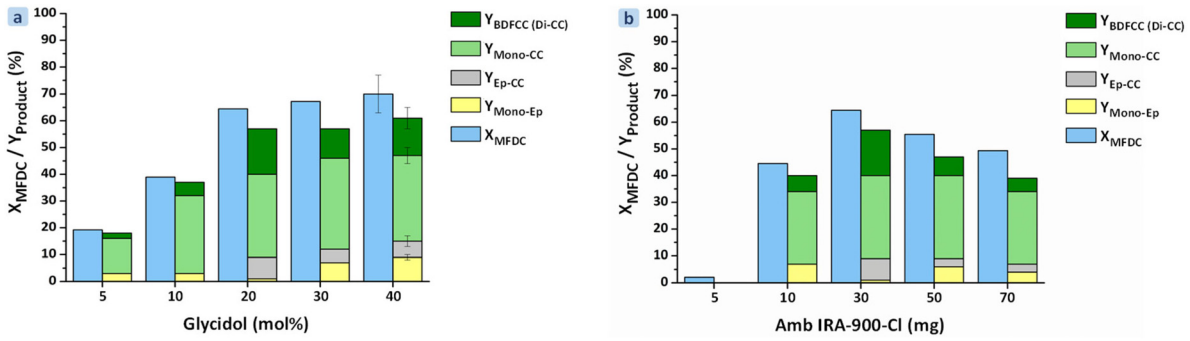


**Fig. 8** Optimisation of: (a) the amount of glycidol; (b) the amount of Amberlite IRA-900-Cl. Conditions: (a) MFDC (1.0 mmol), GlyC (2.2 mmol), Amberlite IRA-900-Cl (30 mg), no solvent, 2 h, 80 °C, 10 ml $min^{-1}$ of $N_2$. The test at 40 mol% of glycidol was performed in quadruplicate. (b) MFDC (1.0 mmol), GlyC (2.2 mmol), Gly (0.2 mmol), no solvent, 2 h, 80 °C, 10 ml $min^{-1}$ of $N_2$.

chloride ratio is probably detrimental for Step 1 in the proposed mechanism (Scheme 1). On the other hand, it is more difficult to explain why increasing the relative loading of the Amberlite catalyst leads to a lower total yield of carbonate-functionalised furanic products (and particularly of the disubstituted product), though it is worth noting that we observed a decrease in the glycerol carbonate mole balance from 97 to 87% with increasing loading of Amberlite (Table S8).

### Upscaled synthesis of BDFCC

After successfully optimising the synthesis of BDFCC under solvent-free reaction conditions, the feasibility of a reaction scale-up was assessed. When the synthesis was performed on our conventional lab scale, 0.18 g of MFDC was used as a starting material (86% yield of BDFCC after 24 h under optimised conditions). When the synthesis was upscaled by a factor of 20 (Fig. S7), the reaction was carried out using 3.6 g of MFDC, which after 66 h led to >99% conversion. Then, an efficient and sustainable work-up process was developed. BDFCC displays two cyclic carbonates groups, which lead to a polarity comparable to that of GlyC, in which BDFCC is thus very soluble. Glycerol carbonate has a high boiling point, which makes it difficult and energy-intensive to separate it from other compounds by distillation.[34] Instead of adopting chromatographic methods that are time-consuming and require large volumes of solvents, we adopted a precipitation technique. Specifically, we developed a precipitation method that exploits water as a green solvent to precipitate BDFCC and extract GlyC into the aqueous phase. In this way, the GlyC/water fraction can be easily separated from the solid BDFCC by vacuum filtration. This method is straightforward and allowed recovering 63% of BDFCC with purity >95% (4.63 g of BDFCC isolated, impurities: glycerol carbonate and Mono-CC). When the synthesis was further upscaled by a further factor of 2, 7.4 g of MFDC led to the production of 14 g of BDFCC, though the efficiency of our separation procedure decreased to 48% (6.9 g of isolated BDFCC).

## Conclusion

In this work, we reported a novel catalytic method to synthesise a fully renewable and industrially relevant FDCA-derived compound characterised by a rigid structure imparted by a furanic core and two cyclic carbonate groups (2,5-bis-dicarboxyl furan cyclic carbonate, BDFCC). This product was achieved *via* the highly atom efficient, one-step transesterification of dimethyl 2,5-furandicarboxylate (MFDC) with glycerol carbonate (GlyC) at mild temperature (80 °C). For the first time, a novel, affordable and metal-free dual catalytic system consisting of heterogeneous Amberlite IRA-900-Cl polymer beads in cooperation with a catalytic amount of glycidol was found to be highly active for the target reaction, resulting in the formation of BDFCC with high yield and selectivity. The thermodynamically-limited nature of this reaction – which was demonstrated by DFT calculations – was circumvented by understanding that using a solvent as commonly done for similar reactions is not necessary. Instead, performing the reaction under a flow of $N_2$ efficiently removed the methanol by-product, thereby shifting the equilibrium concentrations towards the products. Under these solvent-free and thus more sustainable conditions, and after optimising a series of parameters such as the GlyC/MFDC ratio, time, type of gas carrier and gas flow, an optimum BDFCC yield of 86% was achieved. This represents a marked green advance compared to the previous state of the art for this reaction, which achieved 45% yield of BDFCC requiring a double reaction time at the same temperature and employing toluene as solvent and a homogeneous catalyst that is intrinsically more difficult to recover and reuse.[11] In parallel, a screening of the activity of the catalyst components allowed to address their role, which resulted in a proposal for the reaction mechanism involving an anionic chlorohydrin intermediate formed *via* nucleophilic attack of glycidol by the halides contained in the Amberlite resin beads (Scheme 1). Furthermore, the catalytic system showed stable performance upon recycling. Finally, scalability was demonstrated by upscaling the reaction by a factor of 40, achieving an isolated BDFCC yield of 48%. In summary, we introduced a catalytic approach that enables the solvent-free, scalable synthesis of the renewable FDCA-derived bis-cyclic carbonate BDFCC. We expect that this development will facilitate the adoption of this monomer for the production of green polymers.

## Author contributions

G. Berluti: conceptualisation, investigation, data curation, formal analysis, methodology, visualisation, writing – original draft, review & editing; A. Scopano: investigation, data curation, writing – review & editing; G. Galletti: formal analysis, writing – review & editing; E. Otten: investigation, formal analysis, methodology, writing – review & editing; C. Jehanno: funding acquisition, supervision, writing – review & editing; P. P. Pescarmona: conceptualisation, funding acquisition, methodology, project administration, resources, supervision, validation, writing – original draft, review & editing.

## Conflicts of interest

The authors declare no conflict of interest.

## Data availability

The data supporting this article have been included as part of the supplementary information (SI). Supplementary information: green metrics calculation, set-up configuration, DFT calculations, catalyst recyclability, upscaled synthesis configuration, catalyst activity investigation, products identification, quantification by NMR spectroscopy, NMR spectra of the products, FT-IR spectra, SEM images and TGA of the catalyst. See DOI: https://doi.org/10.1039/d5gc06663h.

## Acknowledgements

We thank the PhD student Folkert de Vries for the support and assistance given when using the NMR spectrometers at the University of Groningen and we acknowledge Dr. Jennifer Hong for help with the SEM analysis. Additionally, we want to express our gratitude to the European Union Horizon Europe Research and Innovation program for financing through the Marie Skłodowska-Curie Grant Agreement No. 101073223 (D-Carbonize project) the PhD projects of G. Berluti and A. Scopano.

## References

1 M. Usman, A. Rehman, F. Saleem, A. Abbas, V. C. Eze and A. Harvey, *RSC Adv.*, 2023, **13**, 22717.
2 P. P. Pescarmona, *Curr. Opin. Green Sustainable Chem.*, 2021, **29**, 100457.
3 N. Bragato and G. Fiorani, *Curr. Opin. Green Sustainable Chem.*, 2021, **30**, 100479.
4 F. D. L. Cruz-Martínez, M. M. Sarasa-Buchaca, J. Martínez, J. Fernández-Baeza, L. F. Sánchez-Barba, A. Rodríguez-Diéguez, J. A. Castro-Osma and A. Lara-Sánchez, *ACS Sustainable Chem. Eng.*, 2019, **7**, 20126.
5 L. Zhang, X. Luo, Y. Qin and Y. Li, *RSC Adv.*, 2017, **7**, 37.
6 M. Sajid, X. Zhao and D. Liu, *Green Chem.*, 2018, **20**, 5427.
7 A. J. Kamphuis, F. Picchioni and P. P. Pescarmona, *Green Chem.*, 2019, **21**, 406.
8 Q. Hou, *et al.*, *Green Chem.*, 2021, **23**, 119.
9 M. Annatelli, *et al.*, *Green Chem.*, 2024, **26**, 8894.
10 P. S. Choong, Y. L. E. Hui and C. C. Lim, *ACS Macro Lett.*, 2023, **12**, 1094.
11 G. Shen and B. Andrioletti, *Molecules*, 2022, **27**, 4131.
12 M. Eltayeb, S. Li, P. U. Okoye and S. Wang, *J. Polym. Environ.*, 2021, **29**, 1880.
13 M. R. Monteiro, C. L. Kugelmeier, R. S. Pinheiro, M. O. Batalha and A. Da Silva César, *Renewable Sustainable Energy Rev.*, 2018, **88**, 109.
14 J. Liu, Y. Li, J. Zhang and D. He, *Appl. Catal., A*, 2016, **513**, 9.
15 A. Kostyniuk, D. Bajec, P. Djinović and B. Likozar, *Chem. Eng. J.*, 2020, **394**, 124945.
16 P. Prete, D. Cespi, F. Passarini, C. Capacchione, A. Proto and R. Cucciniello, *Curr. Opin. Green Sustainable Chem.*, 2022, **35**, 100624.
17 R. A. Sheldon, *ACS Sustainable Chem. Eng.*, 2018, **6**, 32.
18 Y. A. Alassmy, Z. Asgar Pour and P. P. Pescarmona, *ACS Sustainable Chem. Eng.*, 2020, **8**, 7993.
19 S. Tanaka, *et al.*, *Chem. Sci.*, 2022, **13**, 4490.
20 L. S. Da Silveira Pinto, E. T. Da Silva and M. V. N. De Souza, *Org. Prep. Proced. Int.*, 2016, **48**, 319.
21 S. Tanaka, *et al.*, *Tetrahedron Lett.*, 2019, **60**, 2009.
22 T. P. Kainulainen, P. Erkkilä, T. I. Hukka, J. A. Sirviö and J. P. Heiskanen, *ACS Appl. Polym. Mater.*, 2020, **2**, 3215.
23 Y. Liu, J. Zhao, Y. Peng, J. Luo, L. Cao and X. Liu, *Ind. Eng. Chem. Res.*, 2020, **59**, 1914.
24 R. K. Henderson, *et al.*, *Green Chem.*, 2011, **13**, 854.
25 F. P. Byrne, *et al.*, *Sustainable Chem. Processes*, 2016, **4**, 7.
26 K. Alfonsi, *et al.*, *Green Chem.*, 2008, **10**, 31.
27 I. B. Jovein, *et al.*, *ACS Eng. Au*, 2025, **5**, 234.
28 S. Grimme, A. Hansen, J. G. Brandenburg and C. Bannwarth, *Chem. Rev.*, 2016, **116**, 5105.
29 S. Gilassi and S. Kaliaguine, *J. Org. Chem.*, 2024, **89**, 7004.
30 A. V. Marenich, C. J. Cramer and D. G. Truhlar, *J. Phys. Chem. B*, 2009, **113**, 6378.
31 Y. A. Alassmy, P. J. Paalman and P. P. Pescarmona, *ChemCatChem*, 2021, **13**, 475.
32 C. Muzyka, D. V. Silva-Brenes, B. Grignard, C. Detrembleur and J.-C. M. Monbaliu, *ACS Catal.*, 2024, **14**, 12454.
33 M. R. Nimlos, S. J. Blanksby, X. Qian, M. E. Himmel and D. K. Johnson, *J. Phys. Chem. A*, 2006, **110**, 6145.
34 A. E. Eisenhart and T. L. Beck, *J. Phys. Chem. B*, 2021, **125**, 2157.

 